

Small-worlds: How and why

Nisha Mathias¹ and Venkatesh Gopal²

¹*Department of Computer Science and Automation, Indian Institute of Science,
Bangalore 560012, INDIA; email: nisha@csa.iisc.ernet.in*

²*Raman Research Institute, Sadashivanagar, Bangalore 560080, INDIA; email:
vgopal@rri.ernet.in*

Abstract

We investigate small-world networks from the point of view of their origin. While the characteristics of small-world networks are now fairly well understood, there is as yet no work on what drives the emergence of such a network architecture. In situations such as neural or transportation networks, where a physical distance between the nodes of the network exists, we study whether the small-world topology arises as a consequence of a tradeoff between maximal connectivity and minimal wiring. Using simulated annealing, we study the properties of a randomly rewired network as the relative tradeoff between wiring and connectivity is varied. When the network seeks to minimize wiring, a regular graph results. At the other extreme, when connectivity is maximized, a near random network is obtained. In the intermediate regime, a small-world network is formed. However, unlike the model of Watts and Strogatz (Nature **393**, 440 (1998)), we find an alternate route to small-world behaviour through the formation of hubs, small clusters where one vertex is connected to a large number of neighbours.

1 Introduction

Coupled systems may be modelled as networks or graphs, where the vertices represent the elements of the system, and the edges represent the interactions between them. The topology of these networks influences their dynamics. Network topologies may be random, where each node or vertex is randomly wired to any other node; or they may be regular, with each vertex being connected to a fixed number of neighbouring nodes. Watts and Strogatz [1] showed that between these two extremes lay another regime of connectivity, which they called a *small-world* network. Such networks are ‘almost’ regular graphs, but with a few long range connections.

What does it mean to have a ‘long-range’ connection? Consider a few examples of networks: neurons in the brain, transportation and social networks, citations of scientific papers and the world wide web. There is a difference between the elements of this list. Social networks, paper citations and the internet, are networks where the links have no physical distance. For example, a link between two websites physically far apart is no different from one between two machines that are next to one another. Neural and transportation networks however, have a well defined

physical distance between their nodes. In this paper, we investigate how placing a *cost* on the length of an edge affects the connectivity of the network.

We now briefly describe the small-world model of Watts and Strogatz (WS) and also introduce the notation that we shall use. WS considered a ring lattice; n sites arranged at regular intervals on a ring, with each vertex connected to k nearest neighbours. Disorder is introduced into the graph by randomly rewiring each of the edges with a probability p . While at $p = 0$, the graph remains k -regular, at $p = 1$, a random graph results. They quantified the structural properties of this lattice by two parameters, L and C . L , the *characteristic path length* reflects the average connectivity of the network, while C , the *clustering coefficient* measures the extent to which neighbours of a vertex are neighbours of each other. Networks exhibiting small-world behaviour are characterized by low characteristic path length, and high clustering coefficient. Finally, we point out that there are two kinds of distances in a graph. One is the *graph* distance, the minimal number of links between any two vertices of the graph. The other is the Euclidean or *physical* distance between these vertices.

Although recent work has shown small-worlds to be pervasive in a range of networks that arise from both natural and man-made technology [1, 2], the hows and whys of this ubiquity have not been explained. The fact that small-worlds seem to be one of nature’s ‘architectural’ principles, leads us to ask what constraints might force networks to choose a small-world topology. We attempt to understand the emergence of the small-world topology in networks where the physical distance is a criterion that cannot be ignored.

2 Can small-worlds arise as the result of an Optimization?

Consider a toy model of the brain. Let us assume that it consists of local processing units, connected by wires. What constraints act on this system? On the one hand, one would want the highest connectivity between the local processing units so that information could be exchanged as fast as possible. On the other, it is wasteful to wire everything to everything else. The energy requirements are higher, more heat is generated, and more material needs to be used, and consequently, more space is occupied. Unrealistic though this model is, it motivated us to examine whether small-worlds would emerge as the result of these constraints.

The concept of multiple scales was introduced by Kasturirangan [3], where he asserted that the fundamental mechanism behind the small-world phenomena is not disorder or randomness, but the presence of edges of many different length scales. The *length scale* of a newly introduced edge e_{ij} , is defined to be the graph distance between vertices i and j *before* the edge was introduced. He argued that the distribution of length scales of the new edges is significantly more important than whether the new edges are long, medium or short range.

We obtain the edge scale distribution by binning the length scales of all the edges in a graph, with respect to its corresponding regular graph. Starting with a k -regular graph, and using

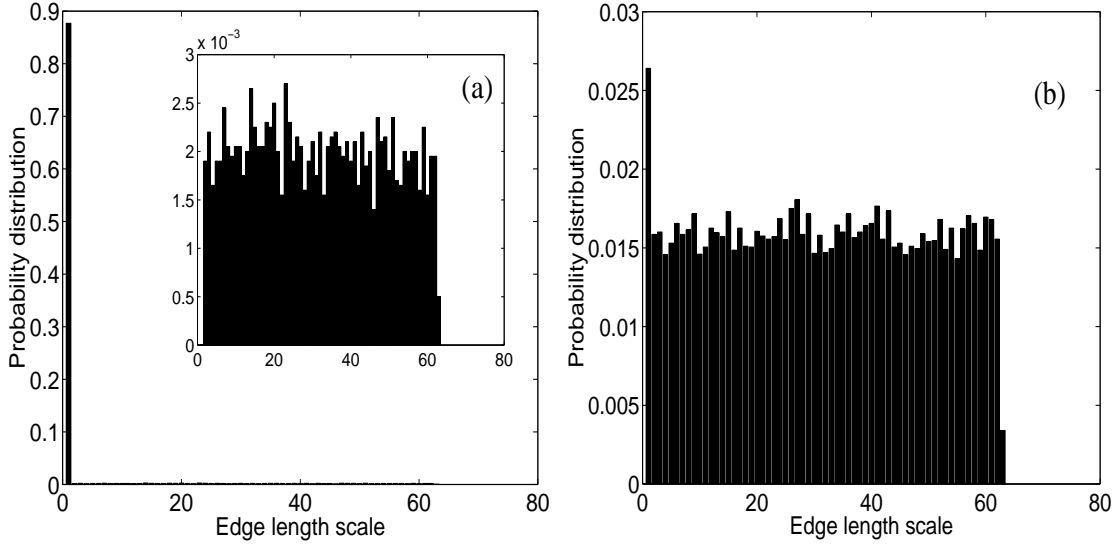


Figure 1: Edge length scale distribution at (a) $p=0.125$, and (b) $p=1.00$; p being the degree of disorder introduced into the $n=250$, $k=4$ regular network using the WS rewiring procedure to introduce small-world behaviour. The inset in (a) displays the distribution of all length scales other than the unit scale. Both plots are averaged over 25 samples.

the WS rewiring procedure, we study the edge scale distribution at various degrees of disorder. Figure 1 shows the edge scale distribution at two degrees of disorder. Figure 1(a) shows the edge scale distribution in the small-world regime, ($p = 0.125$). Due to introduction of a small amount of disorder, a few edges are rewired to become far and consequently have a large length scale. However, they are too few in number to significantly alter the length scale distribution and hence, the edges of unit length scale dominate the distribution. Figure 1(b) shows the edge scale distribution at $p = 1$, a random graph. Here, the edges are uniformly distributed over the entire length scale range, that is, from 1 to n/k . The network still retains a slight bias towards the unit length scale. At both these degrees of randomness however, the characteristic path length scales logarithmically with n . There thus appears to be some factor that constrains the distribution of edge length scales to (a) and not (b), namely, restricting the rewiring to just a few far edges. We question whether the association of a cost to each edge, proportional to its length, serves to work as this constraint.

3 Optimization model

We use the method of simulated annealing [4] to find the network which results in the best optimization of the objective function E , whose minimization is the goal of the procedure. The network used in the model is that of vertices arranged symmetrically along a ring. The size of

the network, n , as well as the total number of edges are fixed. So also are the positions of the vertices, which are equally spaced along the circumference of the circle. Initially, the network is k -regular, similar to the WS model. The configuration has an associated energy E , a function of both its wiring cost and the average degree of separation between its vertices. The objective function E is taken to be,

$$E = \lambda L + (1 - \lambda)W,$$

a linear combination of the normalized characteristic path length L , and the normalized wiring cost W . The characteristic path length L , as defined by Watts and Strogatz, is the average distance between all pairs of vertices, given by

$$L = \frac{1}{n(n-1)} \sum_{i \neq j} d_{ij},$$

where d_{ij} is the number of links along the shortest path between vertices i and j . It is therefore a measure based on graph distance, and reflects the global connectivity among all vertices in the graph. The wiring cost W , in contrast, is a measure of the physical distance between connected vertices. The cost of wiring an edge e_{ij} , is taken to be the Euclidean distance between the vertices i and j . Hence, the total wiring cost is

$$W = \sum_{e_{ij}} \sqrt{(x_i - x_j)^2 + (y_i - y_j)^2},$$

where (x_i, y_i) are the coordinates of vertex i on the ring lattice. The characteristic path length L is normalized by $L(0)$, the path length in the k -regular network; while W is normalized by the total wiring cost that results when the edges at each vertex are the longest possible, namely, when each vertex is connected to its diametrically opposite vertex, and to the vertices surrounding it. The parameter λ is varied depending on the relative importance of the minimization of L and W . One can regard $(1 - \lambda)$ as the wiring cost per unit length, and W as the length of wiring required.

Starting from the initial regular network, a standard Monte Carlo scheme [4] is used to search for the energy minimum. Similar to the WS model, duplicate edges and loops were not allowed, and it was ensured that the rewiring did not result in isolated vertices. The starting value for T , the annealing ‘temperature’, was initially chosen to be the initial energy, E , itself. The temperature was then lowered in steps, each amounting to a 10 percent decrease in T . Each value of T was held constant for 150 reconfigurations, or for 15 successful reconfigurations, whichever was earlier.

4 Optimized Networks: Results

Since minimum characteristic path length, and minimum wiring cost are contradictory goals, the optimization of either one or the other will result in networks at the two ends of the randomization spectrum. As expected, at $\lambda = 0$, when the optimization function concentrates only on minimizing the cost of wiring edges, a regular network emerges with uniform connectivity and high characteristic path length ($L \sim n$). The edge scale distribution shows all edges to be concentrated almost entirely within the unit length scale, as shown in Fig. 2 (a). At $\lambda = 1$, when only the characteristic path length is to be minimized, again of no surprise, the optimization results in a near random network ($L \sim \ln n$). The edge scale distribution shown in Fig. 2 (b) has edges having lengths distributed uniformly over the entire length scale range.

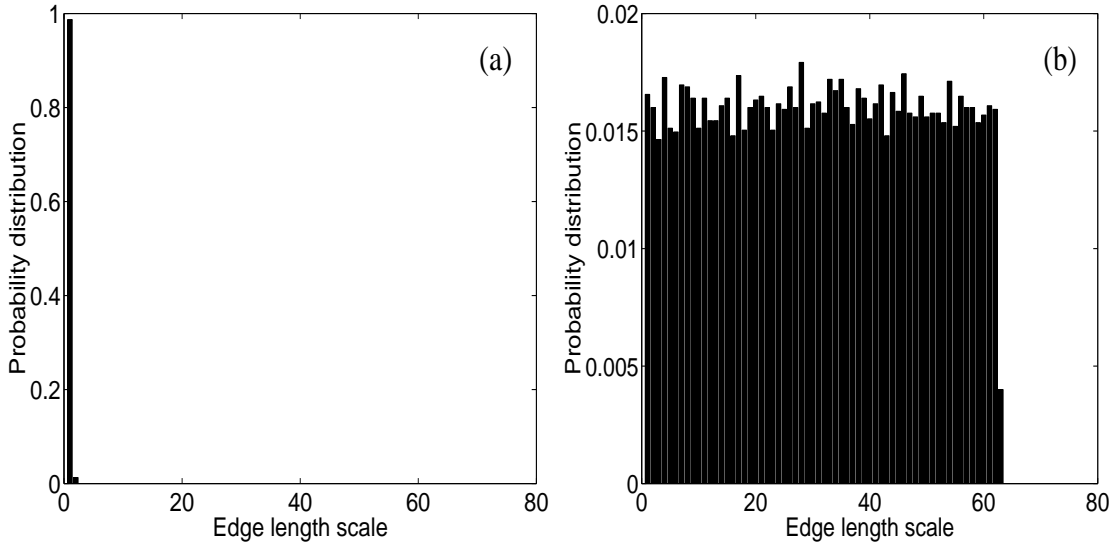


Figure 2: Edge scale distribution resulting from optimization at (a) $\lambda = 0$, and (b) $\lambda = 1$ for a network having $n = 250$, $k = 4$. Both distribution plots are averaged over 25 simulations.

4.1 The emergence of hubs

At intermediate values of λ , the optimization model results in *hubs*, that is, a group of nodes connected to a single node. Due to the constraint which seeks to minimize physical distance between connected vertices, hubs are formed by vertices close to one another. In addition, the minimization of graph distance ensures the existence of connections between hub centres, enabling whole hubs to communicate with each other. The edges at any hub centre therefore, span a wide range of length scales. Hubs emerge due to the contribution of L to the optimization function. The formation of hubs, en route to the emergence of a small-world network, has so far not been reported in the literature.

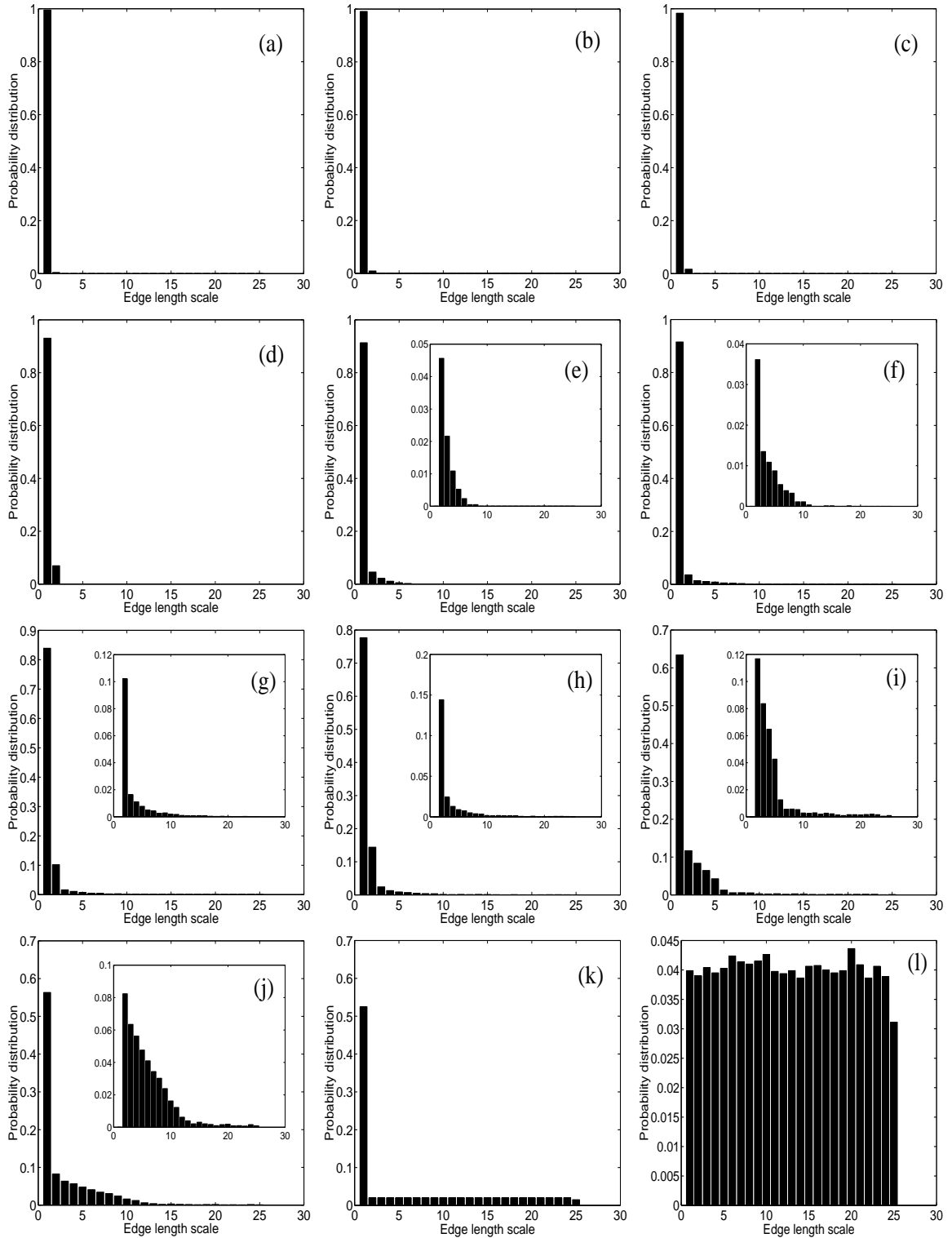


Figure 3: Edge scale distribution for an $n=100, k=4$ network at various λ : (a) 0.0, (b) 5×10^{-4} , (c) 5×10^{-3} , (d) 1.25×10^{-2} , (e) 2.5×10^{-2} , (f) 5×10^{-2} , (g) 1.25×10^{-1} , (h) 2.5×10^{-1} , (i) 5×10^{-1} , (j) 7.5×10^{-1} , (k) 8.5×10^{-1} , (l) 1.0. The inset in each plot shows the distribution of all scales with the unit length scale excluded. Each plot is an average over 40 simulations.

The extreme situation is a ‘universal’ hub: a single node, with all other nodes having connections to it. However, except for the situations when the cost of wiring is negligible, we find that the optimization does not result in a universal hub. This is apparent, since a universal hub requires all the remaining $n - 1$ vertices to have connections to the vertex at the centre of the hub, resulting in length scales which span the entire scale range, long connections being prohibitively expensive. A real world example of such a universal hub network is unlikely since a large hub is a bottleneck to traffic through it, resulting in overcrowding at the hubs [3]. Hence, the need for multiple, and consequently smaller, hubs.

Watts [5] defines the *significance* of a vertex v , as the characteristic path length of its neighbourhood $\Gamma(v)$, in its absence. Hub centres are significant since they contract distances *between* every pair of vertices within the hub. Thus, vertex pairs although not directly connected, are connected via the single common vertex. Hence, the average significance, a measure which reflects the number of contractions, is considerable. Thus, in contrast to the WS model, where networks become small due to shortcuts, here smallness can be attributed to the small fraction of highly significant vertices.

The formation of the universal hub at sufficiently large λ is not surprising, since it can be shown that for a network that minimizes L and employs only rewirings, a universal hub will effect the largest minimization. The formation of *multiple* hubs however is due to the role played by W in the optimization, which is to constrain the physical length of edges, and therefore, the size of hubs. As the hubs grow, whenever the cost of edges from the hub centre to farthest nodes become high, the edges break away resulting in multiple hubs. Thus, high wiring cost prevents the formation of very large hubs, and controls both the size and number of hubs. Figures 4 and 5, demonstrate the evolution of hubs in an $n = 100, k = 4$ optimized network as λ is varied between 0 and 1. While Fig. 4 uses ring-lattice displays to illustrate the evolution, Fig. 5 illustrates the same networks as 2d-displays. In the ring-lattice displays, vertices are fixed symmetrically around the lattice, with hub centres and long-range inter-hub links being clearly visible. The 2d-displays are generated by a graph drawer which uses a spring embedder to clearly demonstrate vertex interconnectivity. Now, with vertices no longer fixed along a ring-lattice, short-range inter-hub links can be distinguished apart from local connectivity.

4.2 Hub evolution

We now detail the evolution of hubs using the edge scale distribution shown in Fig. 3, and hub variation described by Figs. 4 and 5. All three figures show the same $n = 100$ and $k = 4$ network at various λ .

In Figs. 3 and 5(a), the optimization results in a near regular network, with hardly any hubs. When the cost reduces slightly to allow for an increase in edge wiring, small hubs are formed. For increasing, but very small λ , Figs. 3(b-c) show the edges to be almost entirely concentrated in the unit length scale, with very few longer edges. The non-unit length scale edges account

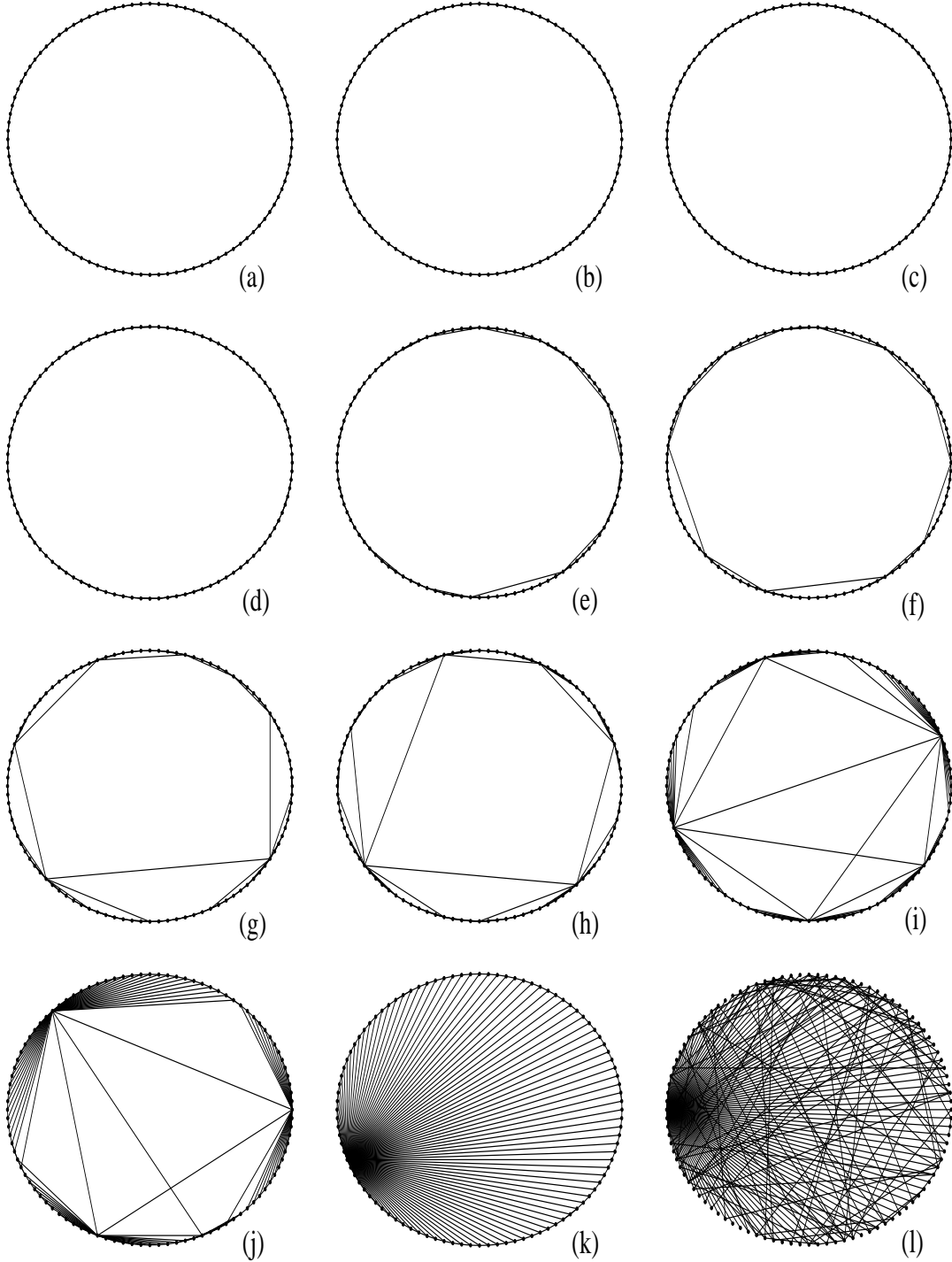


Figure 4: The ring lattice displays illustrate the evolution of hubs as λ is varied over the $[0,1]$ range for an $n = 100, k = 4$ optimized network. Very short inter-hub links cannot be distinguished apart from local vertex connectivity, however longer range inter-hub links are clearly visible. Distinct hub centres illustrate the presence of hubs, as well as their variation in size and number. The single hub centre at the universal hub limit is clearly illustrated. λ : (a) 0.0, (b) 5×10^{-4} , (c) 5×10^{-3} , (d) 1.25×10^{-2} , (e) 2.5×10^{-2} , (f) 5×10^{-2} , (g) 1.25×10^{-1} , (h) 2.5×10^{-1} , (i) 5×10^{-1} , (j) 7.5×10^{-1} , (k) 8.5×10^{-1} , (l) 1.0.

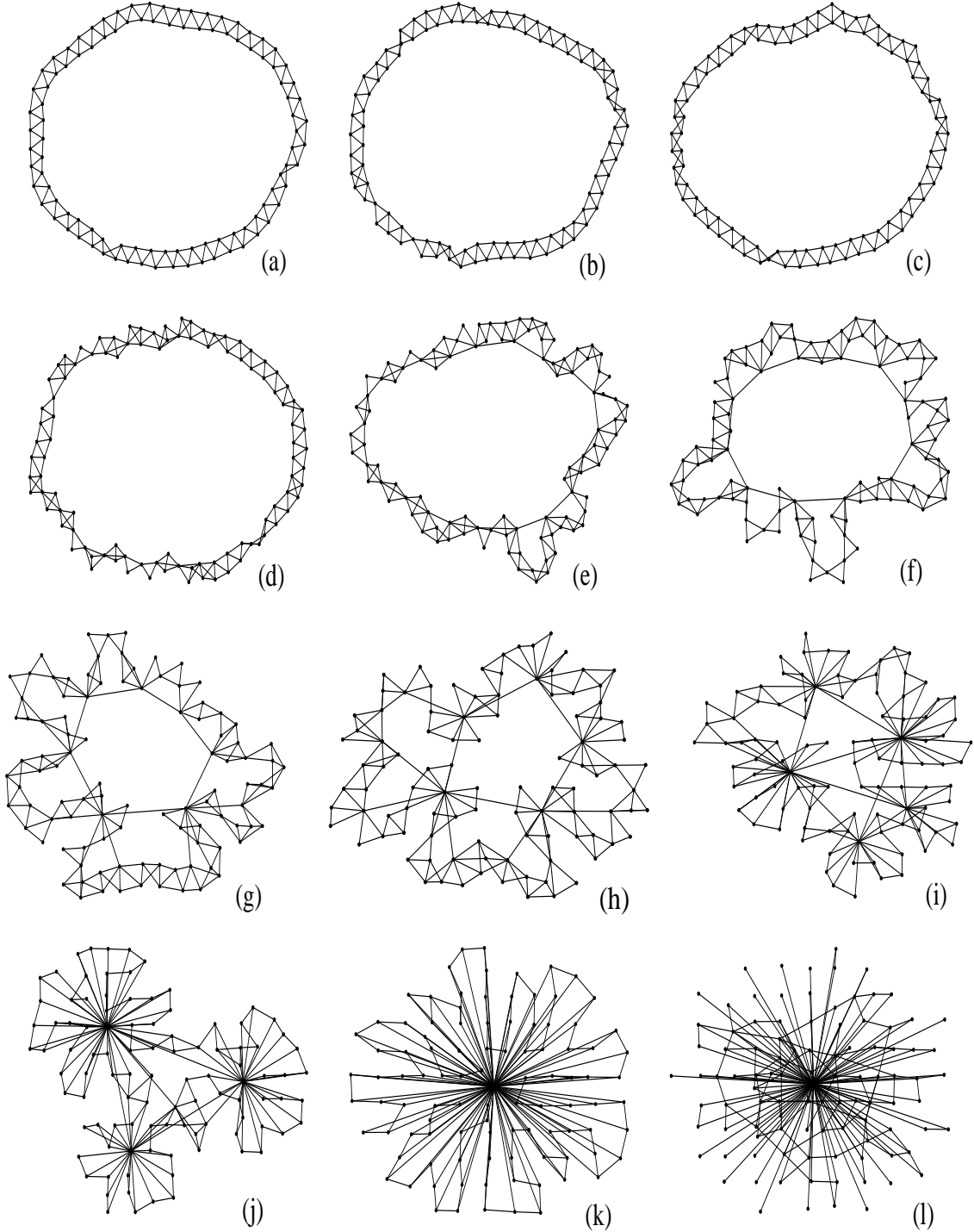


Figure 5: Illustrates the evolution of hubs for an $n = 100, k = 4$ optimized network as λ is varied over the same $[0,1]$ range as the previous figure. The same networks are displayed as 2d-graphs using a graph generator with a spring embedder. Now since vertices are not displayed as being fixed along a ring lattice, vertex interconnectivity, as well as the emergence of hubs and their variation in size and number is well illustrated. λ : (a) 0.0, (b) 5×10^{-4} , (c) 5×10^{-3} , (d) 1.25×10^{-2} , (e) 2.5×10^{-2} , (f) 5×10^{-2} , (g) 1.25×10^{-1} , (h) 2.5×10^{-1} , (i) 5×10^{-1} , (j) 7.5×10^{-1} , (k) 8.5×10^{-1} , (l) 1.0.

for very few and very small hubs, as illustrated in Figs. 5(b-c). Due to their small size, and very short inter-hub links, the hubs are indistinguishable from local vertex connectivity in the ring lattice displays in Figs. 4(a-d).

A slight fall in the wiring cost permits an increased number of hubs. The high cost of wiring constrains hubs to be still rather small. Hence, the distribution of scales in Fig. 3(d) still shows only two length scales. However, there is a marked increase in edges of the second length scale. The effort towards minimizing L , ensures that the few hubs are bunched close together so that short inter-hub links can be used to enable the maximum distance contraction possible (Fig. 5(d)).

When further reduction in cost permits increased wiring, it is mostly the inter-hub links that take advantage of the reduced cost to enable hubs to be scattered over the entire network. Figure 3(e) shows clearly the multiple length scales generated by inter-hub links. The marked increase in the range of the inter-hub links (Fig. 4(e)), allows them for the first time to be visible in the ring-lattice plots. Figure 5(e) shows that there is not much variation in the hub size, except for the longer range of the inter-hub links.

Figures 3 and 4(f-h) demonstrate that as λ increases further, the length and number of far edges are progressively less constrained, and the extended length permits larger and many more hubs. Vertices lose their local nearest-neighbour interconnectivity as hubs centres dominate in connectivity (Figs. 5(f-h)). However, as the size of hubs increases, they are consequently reduced in number. In Figs. 5(i-k) one observes efforts towards a uniform reduced local connectivity. The number of inter-hub links increases to yield greater inter-hub distance contraction.

Figures 5(i-j) are marked by a sharp reduction in the number of hubs as the hubs balloon in size. This evolution culminates in the emergence of the universal hub, (Fig. 5(k)), a single hub of connectivity. The formation of edges between the hub centre, and all the other $n - 1$ vertices, as illustrated in Fig. 4(k), results in a uniform distribution of non-unit length scale edges. Wiring, which is still associated with a cost, albeit small, ensures that the remainder of the edges are entirely local, as can be observed from the distribution in Fig. 3(k).

Figure 4(l) demonstrates that when $\lambda = 1$, the universal hub is retained. However, due to the absence of any effort towards minimal wiring, edges are uniformly distributed across the entire length scale range as shown in Fig. 3(l). The loss in local connectivity can be clearly seen in comparison to Figs. 4 and 5(k). Optimization towards minimizing only L , results in the *re-emergence* of multiple hubs, but the removal of the constraint on wiring allows hubs to be composed of largely non-adjacent vertices.

In conclusion, during the evolution of hubs illustrated in figures (a-l), as the cost of wiring is decreased, the following sequence is seen :

- Hubs emerge, and grow in size and number
- Increase in the range and number of inter-hub links
- Subsequent reduction in the number of hubs

- Formation of a universal hub
- Hubs re-emerge accompanied by a loss in local vertex interconnectivity, while the universal hub remains

5 Optimization and the WS model: Some comparisons

For the remaining part of this section, we present further results, but against the backdrop of the WS model. To define small-world behaviour, two ingredients were used by Watts and Strogatz. The first was the characteristic path length, a global property of the graph, while the second, the clustering coefficient, C , is a local property which quantifies neighbourhood ‘cliquishness’. Associated with each vertex v , is its neighbourhood, Γ_v , the k_v vertices to which it is directly connected, and among which there can be a maximum of $k_v(k_v - 1)/2$ connections. C_v , the clustering coefficient of v , denotes the fraction of the links actually present among its neighbours, defined as

$$C_v = \frac{|E(\Gamma_v)|}{\binom{k_v}{2}},$$

while C is C_v averaged over all v .

The WS and optimization models are compared with respect to their normalized small-world characteristics. In addition, we study their different behaviours with respect to normalized wiring and degree. All results are obtained using an $n = 100, k = 4$ network. Each plot is the result of averaging over 40 simulation runs.

5.1 Characteristic path length

We begin our comparison with the characteristic path length, the parameter whose smallness gives these networks their name. Figure 6 compares L for the WS and optimized models. The control parameters in the two models, λ the optimization parameter, and p the WS parameter, are similar in that they both control the introduction of far edges. It should be remembered though, that while p controls only the *number* of far edges, allowing their length scales to be uniformly distributed across the entire range, λ constrains not only the number, but also the physical *length* of far edges.

In both cases, L shows a sharp drop that signifies the onset of small-world behaviour. However, in contrast to the gradual drop effected by the random assortment of rewired edges in the WS model, the drop due to hub formation is much sharper. Although its initial reduction is smaller due to the additional constraint on edge length, its final value is much lower than the WS random graph limit.

The variation in L resulting from optimization, can be understood from the role played by the hub centres in contracting distance between pairs of vertices. Before the cliff, the hubs being few and very small, effect a very slight distance contraction. The tip of the cliff forms due to a marked increase in hubs, while the sharp drop occurs when extended range inter-hub links yield a pronounced distance contraction between many distant hubs and their widely separated neighbourhoods. The transition from many, small hubs to much larger and consequently fewer hubs, results in the gradual reduction in L . Finally, on the emergence of the universal hub, which has no counterpart in the WS model, the single hub centre contracts the distance between *every* pair of vertices, resulting in an average distance less than 2.

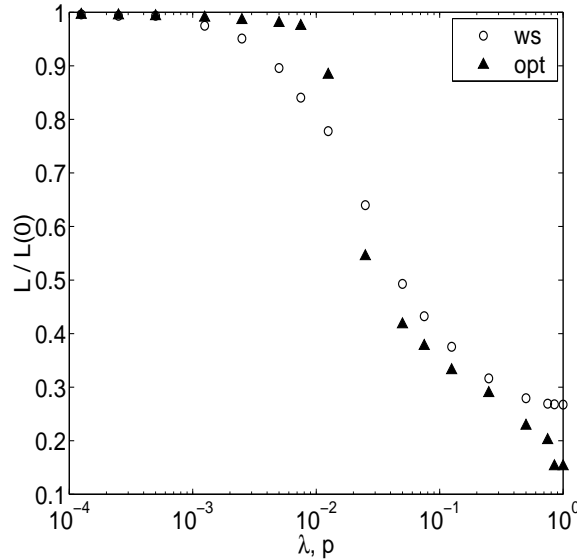


Figure 6: Variation in the normalized characteristic path length, $L/L(0)$, versus p and λ , for the WS model and optimization model respectively.

5.2 Clustering coefficient

Figure 7, which compares the variation in clustering coefficient for the two models, shows far more interesting behaviour. The drop in local connectivity that is seen in the WS model does not occur *at all* for the optimized network because of the formation of hubs. Although the clustering coefficient was not a characteristic that was sought to be maximized, high cliquishness emerges. Figure 7 shows that the formation of hubs sustains the clustering coefficient at a value higher than that for the corresponding regular graph, unlike the WS model. Thus, the similarity between p and λ as control parameters is only valid for L .

Before a more detailed analysis of Fig. 7, we discuss the clustering coefficient further. For a vertex v , its neighbourhood size k_v , plays a significant role. The smaller is k_v , the smaller the

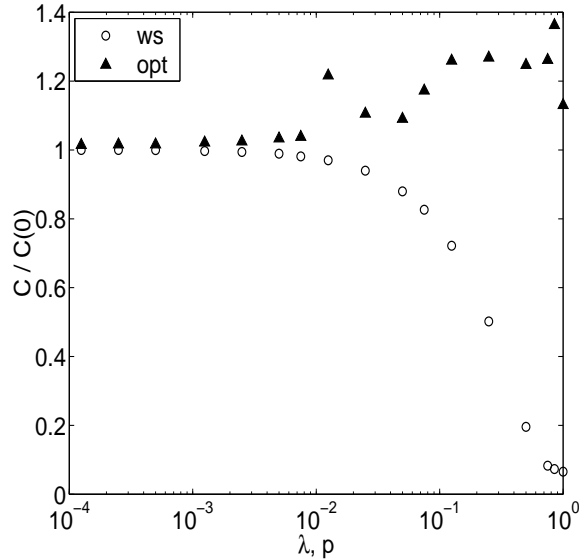


Figure 7: Comparison between the WS model and optimization model with respect to the variation in their normalized clustering coefficient, $C/C(0)$.

number of possible intra-neighbourhood edges. Hence, vertices which lose in connectivity, gain in cliquishness. In a similar manner, vertices which gain in connectivity, lose in cliquishness because of their larger neighbourhood size. This is because, although the vertices have a larger number of intra-neighbourhood edges, they form a smaller fraction of the total number of possible edges. At the universal hub limit, the hub centre has the least clustered neighbourhood owing to the fact that all the remaining $n - 1$ vertices form its neighbourhood. The clustering coefficient can be shown to be approximately $(k - 2)/n$. Although the average degree remains unchanged, the varying hub size and number can influence which neighbourhoods dominate the average clustering coefficient.

In addition, a factor which influences the clustering within neighbourhoods, is the inclusion of a hub centre to a neighbourhood. The effect on clustering differs depending on the range of the link between the vertex and the hub centre. If the range of the link is large and the vertex lies outside the hub, then a far away vertex is being included into an otherwise locally connected neighbourhood. The hub centre has little or no association with the remaining neighbours and so it lowers the average cliquishness. However, if the vertex lies within the hub, it amounts to including a node which is connected to all, or a large fraction of its neighbours. Hence, its neighbourhood becomes more clustered. This effect is more pronounced when (1) the neighbourhood size is small, (2) the vertex includes more than one hub centre in its neighbourhood, and (3) the hub whose centre is being included is composed of largely local neighbours. Thus, unlike L which is tuned by a single parameter, C is controlled by many more, a point that we will return to shortly in the analysis of Fig. 7.

From Fig. 7 we see as expected for the WS model, that $C(p)$ falls as approximately $C(0)(1-p)^3$ [6], and eventually drops almost to zero for the completely randomized graph. This is due to the increasing number of inclusions of random far nodes, into otherwise locally connected neighbourhoods. In contrast, the presence of hubs in the optimization model ensures that $C(\lambda)$ never falls below $C(0)$; reaching its maximum when the network converges to a universal hub.

Keeping in mind the evolution of the optimized network shown in Figs. 4 and 5 we can understand qualitatively the behaviour of $C(\lambda)$ in Fig. 7. When λ is small, the network is dominated by regular neighbourhoods (Fig. (a-c)). As described earlier, vertices adjacent to hub centres gain in cliquishness due to their reduced neighbourhood sizes. Despite there being just a few small hubs, since there are more reduced connectivity vertices than hub centres, the average C is raised slightly above that of a regular graph.

With a slight increase in λ , Figs. 4 and 5(d) shows a sharp increase in C . At this point, the marked increase in hubs, with only a slight increase in size, results in a pronounced increase in the number of reduced connectivity vertices. Many of these vertices have neighbourhoods which are completely clustered (called cliques), since in addition to their reduced size, they include one or more hub centres into their neighbourhood. Cliques, not surprisingly, dominate the average resulting in the large jump in C . However, the emergence of long range inter-hub links in Figs. 4 and 5(e-f) results in lowering C . Their introduction causes: (1) hub centres to have lowered cliquishness owing to the inclusion of distant nodes into their neighbourhoods, and (2) some reduced connectivity neighbourhoods to no longer be complete cliques due to the inclusion of the centre of a hub, which has lost local neighbours to inter-hub neighbours.

Across Figs. 4 and 5(g-h), C rises again due to increased cliques generated not only by the increased number and size of hubs, but also because their larger size allows for the inclusion of local neighbours once again. However, in Figs. 4 and 5(i-k), while the few hubs gain in connectivity (and consequently lose in cliquishness), the remaining vertices veer towards uniformity in reduced connectivity. The resulting marked reduction in the number of cliques, accounts for the slight drop at Figs. 4 and 5(i), while the near uniform reduced connectivity serves to further raise C . Finally, in the universal hub limit, (Figs. 4 and 5(k)), all vertices have a uniform reduced vertex connectivity, at the expense of the single hub centre. Having gained in cumulative connectivity, the hub centre has a very low clustering coefficient of approximately $(k-2)/n$. However, the remaining reduced sized neighbourhoods and their inclusion of the hub centre, ensures the average C shoots up to its maximum.

In Figs. 4 and 5(l), the average clustering falls due to the non-uniformity in vertex connectivity. However the inclusion of the universal hub centre into every neighbourhood ensures C does not drop too much. The multiple hubs result in a variation in vertex connectivity, with hub centres gaining in connectivity at the expense of others. This leaves a few vertices having a *single* connection. With a neighbourhood of only 1, and no intra-neighbourhood connectivity, these vertices are totally unclustered¹ which accounts for the drop in C .

¹Such vertices have $k_v = 1$, and $|E(\Gamma_v)| = 0$, which results in an invalid definition of C_v . Their clustering

Thus, we see an interesting inter-play between neighbourhood size, hub centre inclusions, and the number and range of inter-hub links. However, the data for the variation of C in the optimized model is noisy, mainly because k is very small. Constraints in computational resources have forced us to work with small n . Further, to maintain the sparseness condition of $n \gg k$, a low k was used, which does not really satisfy the WS condition that $k \gg 1$. Due to the small k , even a small loss in connectivity, can cause neighbourhood cliquishness to rise sharply. Although different factors come into play during the C variation, the spikes are due to the pronounced effect of reduced connectivity neighbourhoods, and in particular to those of cliques. The cliques serve to maintain the entire C variation higher than would probably result for higher k . Work is in progress to obtain data using large k networks.

5.3 Wiring cost and Degree

Figure 8(a) displays the increase in the cost of wiring, or alternatively, the amount of wiring, with p and λ . The comparison between the optimization model and WS model illustrates clearly the difference made by the inclusion of the minimal wiring constraint. For small λ , both models exhibit similar wiring cost. At larger λ however, the absence of a similar constraint in the WS model results in a much greater amount of wiring. The clear advantage exhibited by the optimized networks persists until $\lambda = 1$, when optimization neglects the minimization of wiring cost entirely. At this point, the optimized network uses greater wiring than its WS counterpart, but only slightly.

In contrast to the WS model, a constraint on degree is not maintained in the optimized model. Figure 8(b) shows how the maximum degree increases with λ and p , for the two models. The maximum degree, D , is normalized by the network size, n . For the optimized network, D is equivalent to the size of the largest hub. At small λ , there is no difference between the two models, but once hubs begin to emerge, D increases sharply for the optimized network. At both the universal hub, and the near random graph limit, the maximum degree is $(n - 1)$, the size of the universal hub. In contrast, each edge being rewired only once in the WS model allows for only a slight variation in degree. One also observes a similarity in the variations of W and D for the optimized networks, since W controls the size of hubs, and hence D .

5.4 Edge scale distribution

Since the WS rewiring mechanism exercises no restraint on the length scales of the rewired edges, the rewired edges are correspondingly uniformly distributed over the entire length scale range. In contrast, for the minimally wired networks, lower length scales occur with a higher probability.

coefficient can be taken to be either 0 or 1. To be noted, is that rather than 0, a value of 1 would result in the average clustering coefficient being higher than that at the universal hub.

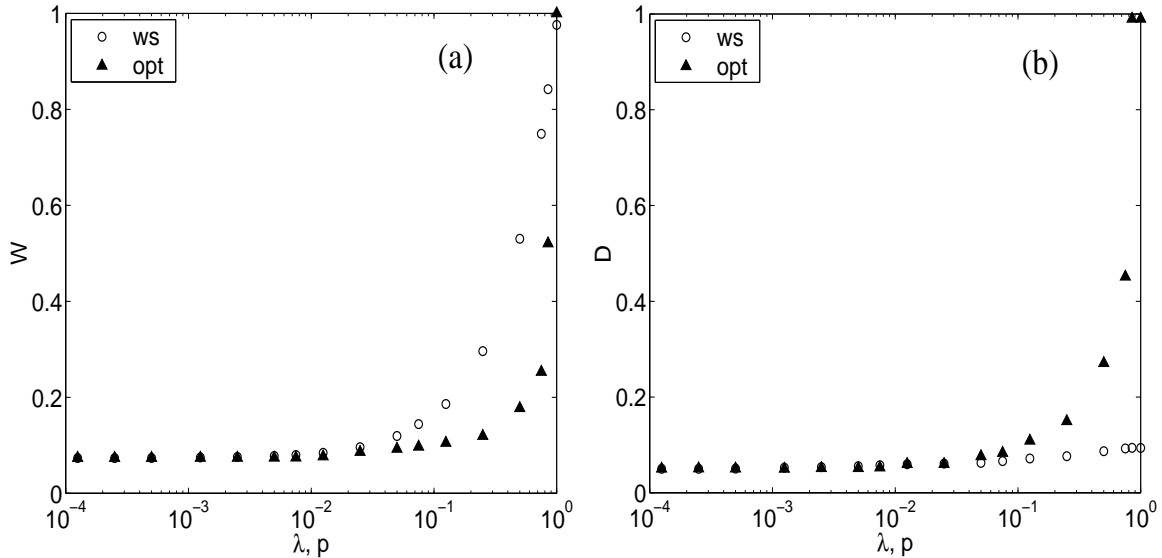


Figure 8: Comparison between the WS and optimization models versus p and λ respectively. (a) Variation in the wiring cost, W , normalized by the optimized value of $W(1)$. (b) Variation in the maximum degree, D , normalized by network size, n . D is equivalent to the size of the largest hub in the optimization model.

Figure 9 shows plots of the edge scale probability distribution on a log-log scale, where a power-law behaviour is seen. Figure 9(a) and (b) illustrate the edge scale distributions at varying λ , while 9(c) is a combined plot which demonstrates the variation in the power-law distributions with λ . Each distribution is displayed along with its associated linear least-squares fit. The variation in their exponents, as obtained from the linear least-squares fit to the data against λ , is shown in Fig. 9(d).

The variation in the power law exponents with λ , can be clearly demarcated into two regions. The first, spanning two orders of magnitude variation in λ , exhibits a very slight exponent variation. Figure 9(a) illustrates the typical probability distribution in this regime. Just two points emerge, since the high wiring cost constrains almost all edges to have a unit length scale, with a very slight probability of a higher length scale. A sharp jump in the exponent marks the beginning of the second regime. Figure 9(b) illustrates the typical probability distribution in this regime. It is seen that a straight line is a reasonably good fit to the data over a wide edge scale range. Finally, when $\lambda = 1$ and a near random network is achieved, a flat distribution of length scales results with each scale being equally probable. The combined plot of all the distributions with their associated least-squares fits, although noisy, illustrates the behaviour of the data (Fig. 9(c)).

The exponent variation clearly reveals two regimes of behaviour. The first jump in the exponent corresponds to the onset of small-world behaviour, the first perceptible reduction in L that is

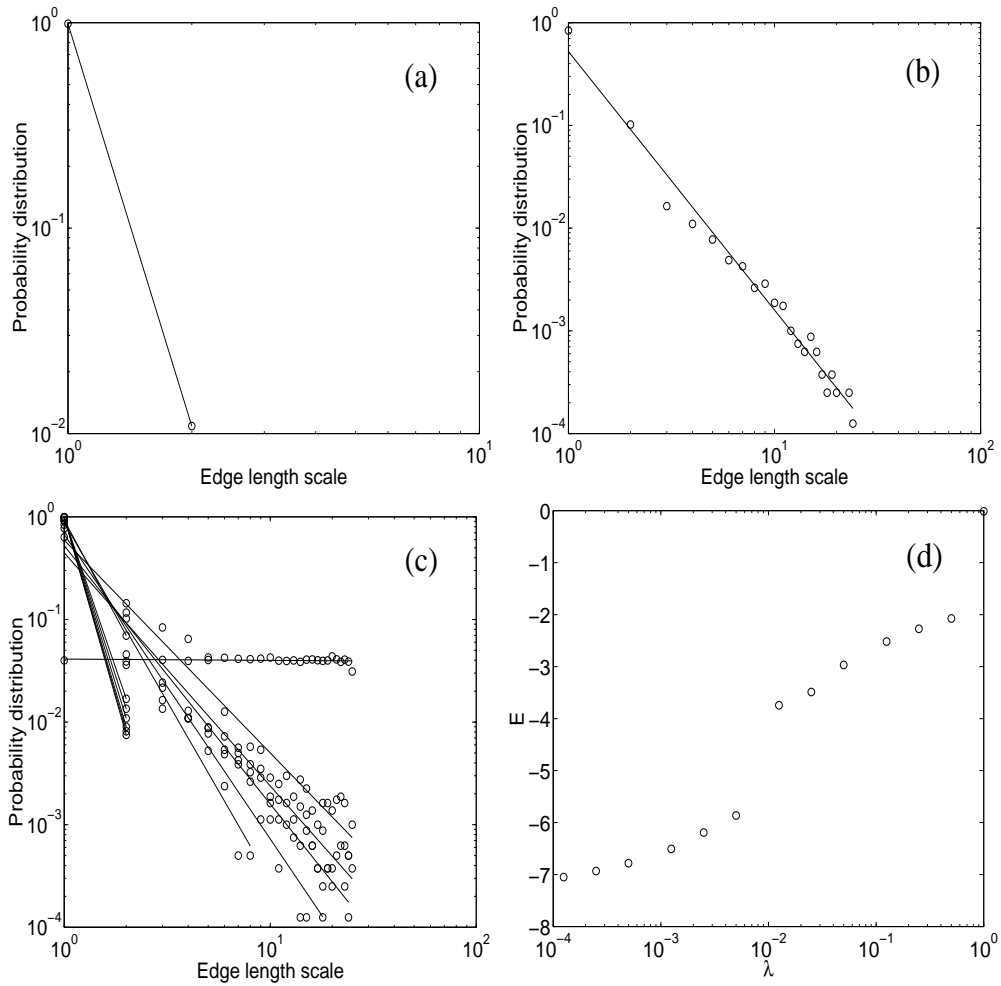


Figure 9: Log-log plot of the edge scale probability distribution at (a) $\lambda = 0.00125$, and (b) $\lambda = 0.125$, for an $n = 100, k = 4$ optimized network. (c) Combined plot of the probability distributions, each with its associated linear least-squares fit. (d) Variation in the power-law exponents with λ . Each distribution plot is averaged over 40 realizations.

seen in Fig. 6. This marks the beginning of the multiple scale regime, and is also a signature of hub formation. As we have mentioned previously, due to computational constraints we were unable to investigate larger networks. We believe that the noise in the data is due to the small size of the networks that we have studied.

Finally, we wish to comment upon Kasturirangan’s multiple scale hypothesis. Figure 9(d) demonstrates clearly the connection between the onset of small-world behaviour and the emergence of multiple length scales in the network. This clearly supports the claim in [3] that small-worlds arise as a result of the network having connections that span many length scales, and forms the first quantitative support of his hypothesis. It is to be noted that multiple scales contribute to reducing L in the WS model as well. However, since no restriction on the length of edges exists, *any* non-zero p will result in multiple scales. Hence, the onset of small-world behaviour appears with a smooth reduction in L .

We have also observed a power law tail for vertex connectivity. We found that most vertices had a small degree, and some were well short of the average degree, with vertices at hub centres gaining at their expense. Owing to the small network size however, the scaling range was rather limited, and so we have not included these results.

6 Do similar networks exist?

Any efficient transportation network works under a similar underlying principle of maximizing connectivity while ensuring that the cost is minimized. Our results seem to indicate that any efficient transportation network will be a small-world, and in addition will exhibit a similar hub connectivity. In a clear illustration of the underlying principle, any map of airline routes, or roadways shows big cities as being hubs of connectivity. This is hardly surprising though, since in such networks, a conscious effort is made toward such a minimization. However, the same philosophy may well be at work in natural transportation and other biological networks.

We would also like to point out that our observed hub structure can be seen in a number of large complex networks ranging from fields as diverse as the world wide web to the world of actors. Kleinberg et al. [7] have observed the following recurrent phenomena on the web: For any particular topic, there tend to be a set of “authoritative” pages focused on the topic, and a set of “hub” pages, each containing links to useful, relevant pages on the topic. Also, it has been noted in [8] that the small-world phenomenon in the world of actors arises due to “linchpins”: hubs of connectivity in the acting industry that transcend genres and eras. In addition, Barabási and Albert [2] explore several large databases describing the topology of large networks that span a range of fields. They observe that independent of the system and the identity of its constituents, the probability $P(k)$ that a vertex in the network interacts with k other vertices decays as a power-law, following $P(k) \sim k^{-\gamma}$. The power law for the network vertex connectivity indicates that highly connected vertices (large k) have a large chance of occurring, dominating the connectivity; hence demonstrating the presence of hubs in these

networks. Thus, hubs seem to constitute an integral structural component of a number of large and complex random networks, both natural and man-made.

7 Conclusions

Watts and Strogatz showed that small-worlds capture the best of both graph-worlds: the regular and the random. There has however been no work citing reasons for their ubiquitous emergence. Our work is an step in this direction, questioning whether small-worlds can arise as a tradeoff between optimizing the average degree of separation between nodes in a network, as well as the total cost of wiring.

Previous work has concentrated on small-world behaviour that arises as a result of the random rewiring of a few edges with no constraint of the length of the edges. On introducing this constraint, we have shown that an alternate route to small-world behaviour is through the formation of hubs. The vertex at each hub centre contracts the distance between every pair of vertices within the hub, yielding a small characteristic path length. In addition, the introduction of a hub centre into each neighbourhood serves to sustain the clustering coefficient at its initially high value. We find that the optimized networks have $C \geq C_{regular}$, and $L \leq L_{random}$ and thus do better than those described by Watts and Strogatz.

In summary, our work lends support to the idea that a competitive minimization principle may underly the formation of a small-world network. Also, we observe that hubs could constitute an integral structural component of any small-world network, and that power-laws in edge length scale, and vertex connectivity may be signatures of this principle in many complex and diverse systems.

Finally, in future work, we will be studying larger networks that were computationally inaccessible to us at present. We are also investigating the application of the small-world architecture in the brain, and also, a dynamic model will be considered to understand the emergence of small-worlds in social networks.

Acknowledgements

N.M. thanks V. Vinay for very useful discussions.

References

- [1] Watts, D. J. and Strogatz, S. H. *Collective Dynamics of ‘small world’ networks*. Nature, 393:440-442, 1998.

- [2] Barabási, A.-L. and Albert, R. *Emergence of Scaling in Random Networks*. cond-mat/9910332.
- [3] Kasturirangan, R. *Multiple Scales in Small-World Graphs*. cond-mat/9904055.
- [4] Press, W. H., Teukolsky, S. A., Vetterling, W. T. and Flannery, B. P. *Numerical Recipes in C: The Art of Scientific Computing*. Cambridge University Press, Second Edition, 1988.
- [5] Watts, D. J. *Small Worlds: The Dynamics of Networks between Order and Randomness*. Princeton University Press, 1999.
- [6] Barrat, A. and Weigt, M. *On the properties of small-world network models*. cond-mat/9903411.
- [7] Kleinberg, J. M., Kumar, R., Raghavan, P., Rajagopalan, S. and Tomkins, A. S. *The Web as a Graph: Measurements, Models, and Methods*. Asano, T. et al. (eds.): COCOON '99, LNCS 1627, 1-17, Springer-Verlag Berlin, Heidelberg, 1999.
- [8] Matthews, R. *Get connected*. New Scientist, 4 December 1999.